BMC Public Health

RESEARCH

Open Access

Exploring the spatiotemporal effects of meteorological factors on hand, foot and mouth disease: a multiscale geographically and temporally weighted regression study

Chao Zhang[1,2†], Zengqiang Kou[3†], Xianjun Wang[3], Fenfen He[4], Dapeng Sun[3], Yan Li[3], Yiping Feng[3], Yongxiao Zheng[1,2], Rongguo Zhang[1,2] and Yunxia Liu[1,2,5*]

Abstract

The influence of meteorological factors on hand, foot, and mouth disease (HFMD) is not on the same scale, it's rare for previous studies to measure and recognize the independent regression relationship between each variable in space and time scale. This study used a multiscale geographically and temporally weighted regression (MGTWR) model to explore the relationship between the incidence of HFMD and related meteorological factors in Shandong Province, China, during 2015–2019 and attempted to quantify the influence of meteorological factors on HFMD under different spatiotemporal effects. Meanwhile, we used the Global Moran's I statistic and Local Moran's I statistic to test the spatial autocorrelation of the incidence of HFMD. HFMD had spatial autocorrelation at the county level in Shandong Province. The MGTWR model outperformed the OLS and GTWR models in determining the relationship between meteorological factors and HFMD. The study highlights significant spatiotemporal non-stationarity in the relationship between meteorological factors and HFMD. Temperature was predominantly positively correlated with HFMD, especially in the peninsula region during spring and summer. Humidity exhibited a predominantly positive correlation, especially in the Shandong Peninsula. Precipitation also showed a positive correlation with HFMD, particularly in western regions and during the winter months. Wind speed had a predominantly negative correlation with HFMD in the central and southwestern regions. The results might help public health authorities set priorities for targeted prevention and control measures in different regions and weather conditions, and provide guidance for the government to rationally allocate public health resources.

Keywords HFMD, Meteorological factors, Moran's I, MGTWR, Spatiotemporal heterogeneity

†Chao Zhang and Zengqiang Kou contributed equally to this work.

*Correspondence:
Yunxia Liu
yunxialiu@163.com
[1]Department of Biostatistics, School of Public Health, Cheeloo College of Medicine, Shandong University, Jinan, Shandong 250012, China
[2]Institute for Medical Dataology, Cheeloo College of Medicine, Shandong University, Jinan, Shandong 250000, China
[3]Shandong Center for Disease Control and Prevention, Jinan, China
[4]Department of Epidemiology and Statistics, Bengbu Medical College, Bengbu, China
[5]Climate Change and Health Center, Shandong University, Jinan, Shandong Province, P.R. China

Introduction

Hand, foot, and mouth disease (HFMD) is a common communicable disease usually affecting children, particularly those aged 5 years and younger [1]. It is caused by many enteroviruses, of which enterovirus 71 (EV-A71) and coxsackievirus A16 (CV-A16) are the most common [2]. Its typical clinical symptoms are a high fever or blister rash on the hands, feet, mouth, or buttocks [3, 4]. In China, HFMD was classified as a class C notifiable infectious disease on May 2, 2008 [5]. More than 18 million HFMD-related cases were reported in Chinese mainland from 2008 to 2017, and the number of deaths has ranked in the top three among all notifiable diseases since 2010 [6]. However, there is still a lack of specific therapeutic drugs. A monovalent HFMD vaccine against EV-A71 has been marketed in China since 2016, but the incidence of HFMD remained high in 2020 [7]. Therefore, it could be very important to explore the main possible risk factors of HFMD for its prediction and control.

Numerous studies have shown that meteorological changes have a substantial impact on the incidence and transmission dynamics of HFMD. For example, higher temperatures and humidity levels are often associated with increased HFMD incidence, possibly because these conditions are conducive to the survival and spread of the virus [8]. Precipitation and wind speed have also been found to significantly affect HFMD transmission, particularly in humid environments and favorable wind speeds, facilitating the spread of the virus among populations [9, 10]. Meanwhile, studies have also demonstrated that the incidence of HFMD is non-stationary in time and space [11]. Therefore, it is essential to study the spatial and temporal variation patterns of the influence of meteorological factors on HFMD to understand the transmission mechanism of the disease and take necessary preventative measures. Moreover, to optimize the timely allocation of health resources, it is also crucial for public health departments to detect the epidemic and its spatial-temporal patterns.

In recent years, many spatiotemporal models have been widely used to explore the temporal or spatial heterogeneity of HFMD. Hong et al. used geographically weighted regression (GWR) to explore the potential risks of HFMD in the Inner Mongolia Autonomous Region of China [12]. Yi et al. used geographically and temporally weighted regression (GTWR) to explore the spatial-temporal characteristics of HFMD and its relationship with meteorological factors in the Ili river valley region of China [13]. The modeling process of classical GWR operates on the same spatial scale, setting the same spatial bandwidth for each variable [14]. This assumption disregards the scale differences between variables. Similarly, the GTWR model only applies a fixed spatial-temporal bandwidth when calibrating regression relationships, treating it as a weighted average of different levels of spatial and temporal heterogeneity [15]. In recent years, traditional GWR and GTWR have been extensively applied in the field of infectious diseases [16–19]. Based on the above two models, Wu et al. studied the multiscale geographically and temporally weighted regression (MGTWR) model and proposed that in order to measure and identify the scale of different processes and quantify the level of spatiotemporal heterogeneity [20], it is necessary to integrate spatiotemporal information into the weighted matrix to study spatiotemporal models at different scales. Previous studies have shown that the spread of HFMD is closely related to meteorological factors such as temperature and humidity [7], precipitation [21], sunshine hours [22], air pressure [23], and wind speed [24], as well as seasonal factors [25], and the influence of these factors is definitely not on the same scale. MGTWR with a flexible bandwidth can compensate for GTWR when measuring and recognizing independent regression relationships between variables at space and time scales.

In this study, we attempted to explore the spatial and temporal heterogeneity of the incidence of HFMD and quantify the influence of meteorological factors on HFMD at different spatiotemporal scales. First, the Global Moran's I statistic and Local Moran's I statistic were used to investigate the spatial autocorrelation of HFMD. Second, the MGTWR model was introduced to analyze the relationship between HFMD and meteorological factors. Meanwhile, the MGTWR model was compared with the ordinary least squares (OLS) model and the GTWR model to verify its significant improvement in model fitting and explanatory power. Third, the spatiotemporal heterogeneity of the effects of meteorological factors on HFMD was displayed at the county scale.

Methods

Study area

Shandong Province, with a total area of 158,000 km^2, is located in eastern China, 34°25′ to 38°23′ N latitude and 114°36′ to 122°43′ E longitude. Shandong has a resident population of nearly 100 million, ranking second in China, which contributes to the high incidence and rapid spread of HFMD. The high population density, particularly in urban areas, facilitates the transmission of the virus among children and exacerbates the severity of the outbreak [26]. Shandong is characterized by a diverse landscape that includes the densely populated North China Plain, the mountainous regions in the central and eastern parts, and an extensive coastline. The varied terrain affects local climate conditions, which in turn influence the transmission dynamics of HFMD. The climate belongs to the warm-temperate monsoon climate, with four distinct seasons, concentrated precipitation,

rain and heat occurring at the same time, short spring and autumn, and long winter and summer. The corresponding relationship between month and season was spring (March - May), summer (July - August), autumn (September - November), and winter (December - February). The geographical and climatic diversity of Shandong makes it an ideal region for studying the impact of meteorological factors on HFMD incidence, which can provide information for public health strategies and interventions in similar regions.

Given that the county administrative level is usually used for HFMD decision-making in China [27], the county was chosen as the spatial analysis unit in this study. Shandong includes 16 municipal districts and a total of 137 subdistricts (counties) (Fig. 1). The geographic information of each county, such as longitude and latitude, was collected from the National Center for Earth System Science and Data (http://www.geodata.cn/).

HFMD and demographic data

Data on HFMD cases were extracted from the China Information System for Disease Control and Prevention (CISDCP). The diagnosis of HFMD was based on the clinical criteria in the HFMD Control and Prevention Guide provided by the Chinese Ministry of Health [28]. As a notifiable disease, all probable and confirmed HFMD cases must be reported online to CISDCP using a standardized form within 24 h of diagnosis. According to the preliminary analysis, more than 99% of reported HFMD cases were less than 15 years old, so this study only included cases under 15 years old reported in Shandong Province from 2015 to 2019. Meanwhile, we defined the population aged 0–15 in each county as a high-risk group.

It was more reasonable to use the monthly cumulative incidence (CI), which was defined as the ratio of the number of monthly reported HFMD cases to the size of the population at risk in the county. However, there were some months in the dataset where no cases occurred at the county level. Zero values can lead to biased parameter estimates. In models such as Poisson distribution, zero values may result in underestimation of the risk probability. When zero values are prevalent, the model may underestimate the actual disease risk, thereby affecting disease prevention and control strategies. Additionally, the presence of zero values can lead to instability during model fitting and affect the convergence of model parameters. Therefore, we used a hierarchical Bayesian model to adjust the crude CI of HFMD [29, 30]. This model included both unstructured and structured random effects to account for spatial and temporal variations

Fig. 1 The location of the study area, Shandong Province in China.(Sources: http://www.geodata.cn/, the map was edited using ArcGIS 10.8)

in the data. The model was implemented using Markov Chain Monte Carlo (MCMC) simulations in WinBUGS 1.4.3, with a burn-in period of 6000 iterations to ensure convergence. The posterior distributions of the model parameters were obtained from the MCMC simulations. Specifically, we used the posterior means of the adjusted cumulative incidence (CI_A) as the dependent variable in the MGTWR model. The CI_A represents the monthly incidence rates of HFMD adjusted for spatial and temporal random effects. Details on the method are provided in Text A in the Supplementary Materials.

Meteorological data

The monthly meteorological data were obtained from the China Meteorological Data Sharing Service System (https://data.cma.cn/), including average temperature (AT, ℃), average relative humidity (ARH, %), average air pressure (AP, KPa), total precipitation (TP, mm), average wind speed (AWS, m/s), and total sunshine hours (SH, h). In order to eliminate the influence of units, meteorological factors were standardized.

Model building

GTWR model

Huang et al. proposed the GTWR model [15], it can be expressed as follows:

$$Y_i = \beta_0(u_i, v_i, t_i) + \sum {}_k\beta_k(u_i, v_i, t_i)X_{ik} + \epsilon_i$$

Where Y_i and X_{ik} are the response variable and the explanatory variables of each space-time location $i(i = 1,2,\ldots,n)$, respectively. $\beta_0(u_i, v_i, t_i)$ is the constant of the point i, $\beta_k(u_i, v_i, t_i)$ is the regression coefficient of the $k^{th}(k = 1,2,\ldots,m)$ explanatory variable at the point i.

Similarly, the $\beta_k(u_i, v_i, t_i)$estimation can be expressed as follows:

$$\widehat{\beta}(u_i, v_i, t_i) = \left[X^T W(u_i, v_i, t_i) X\right]^{-1} X^T W(u_i, v_i, t_i) Y$$

where $W(u_i, v_i, t_i) = diag(\alpha_{i1}, \alpha_{i2}, \ldots, \alpha_{in})$ and n is the number of observations. Here the diagonal elements $\alpha_{ij}(1 \le j \le n)$ are space-time distance functions of (u, v, t) corresponding to the weights when calibrating a weighted regression adjacent to observation point i.

Given a spatial distance d_{ij}^S and a temporal distance d_{ij}^T, we can combine them to form a space-time distance d_{ij}^{ST}, which can be expressed as:

$$d_{ij}^{ST} = \lambda d_{ij}^S + \mu d_{ij}^T$$

Where $(d_{ij}^S)^2 = (u_i - u_j)^2 + (v_i - v_j)^2$, $(d_{ij}^T)^2 = (t_i - t_j)^2$, λ and μ are scale factors in their respective metric systems, respectively, to balance the different influences used to measure spatial and temporal distance. Using Euclidean distance and Bi-square Kernel function to construct a space-time weight matrix, we will have

$$d_{ij}^{ST} = \lambda \left[(u_i - u_j)^2 + (v_i - v_j)^2\right] + \mu (t_i - t_j)^2$$

Where t_i and t_j are observed times at locations i and j.

$$\alpha_{ij} = \begin{cases} \left(1 - \left(\frac{d_{ij}^{ST}}{h_{ST}}\right)^2\right)^2, & if\ d_{ij}^{ST} \le h_{ST} \\ 0, & otherwise \end{cases}$$

Where $(d_{ij}^S)^2 = (u_i - u_j)^2 + (v_i - v_j)^2$, $(d_{ij}^T)^2 = (t_i - t_j)^2$, h_{ST} is the parameters of spatiotemporal bandwidths, respectively. The relationship between different bandwidths can be expressed as:

$$h_S^2 = h_{ST}^2/\lambda,\ h_T^2 = h_{ST}^2/\mu$$

h_S, h_T are the parameters of spatial and temporal bandwidths, respectively. Let τ denote the parameter ratio μ/λ and $\lambda \ne 0$. The essential effect of τ is to match spatial distance by enlarging or reducing the effect of temporal distance. Without loss of generality, previous studies usually set $\lambda = 1$ to reduce the number of parameters in practice.

MGTWR model

The MGTWR model is an extension of the GTWR model by Wu et al. [20], can be expressed as follows:

$$Y_i = \beta_{bwt_0 - s_0}(u_i, v_i, t_i) + \sum_{k=1}^{m} \beta_{bwt_k - s_k}(u_i, v_i, t_i) X_{ik} + \epsilon_i$$

where (u_i, v_i, t_i) denotes the space-time coordinates of the point $i(i = 1,2,\ldots,n)$ in space, t_i is the observation time, Y_i is the dependent variable at the point i, and X_{ik} is the $k^{th}(k = 1,2,\ldots,m)$ explanatory variable at the point i, $\beta_{bwt_0 - s_0}(u_i, v_i, t_i)$ is the regression constant of the point i, $\beta_{bwt_k - s_k}(u_i, v_i, t_i)$ is the regression coefficient of the k^{th} explanatory variable at the point i, bwt_{k-S_K} is the spatiotemporal bandwidth calculated for the k^{th} regression relationship based on the specific temporal bandwidth bwt_k and spatial bandwidth bws_k. The modeling of MGTWR is similar to the GTWR mentioned in Sect. 2.4.1.

Model calibration

For the GTWR model, we selected the optimal bandwidths based on the corrected Akaike Information Criterion (AICc) [31]. The MGTWR model was calibrated using the back-fitting method of maximum likelihood

estimation [32]. When the change of score (SOC) between each successive iteration was small enough, the iteration of MGTWR terminated. SOC was compared with δ, and this study defined $\delta=10^{-3}$ for MGTWR calibration. If SOC<δ, the model iteration was terminated, and the estimated coefficients of the last iteration were the final estimated coefficients. In addition, the maximum spatial scale was initially estimated based on the geographic distribution of the study region, while the maximum temporal scale was defined by the period of data collection. Details on the methods and calculations for bandwidth selection are provided in Text B in the Supplementary Materials.

Statistical analysis

Firstly, the Global Moran's *I* [33, 34] was used to detect the global spatial autocorrelation of the incidence of HFMD. The Local Moran's I was then performed to determine the local spatial autocorrelation of the incidence of HFMD. Secondly, three models, including OLS, GTWR, and MGTWR, were constructed. R^2, adjusted R^2, AICc, and root mean square error (RMSE) were used to evaluate the goodness-of-fit of the model. Thirdly, we conducted a hypothesis test, assuming that all independent variables were non-stationary, and established the *F* statistic [35] to detect the space-time variation of the coefficients. Finally, the pseudo-t test was used to test the significance of the estimated local parameters [36], and the regions with significant coefficients ($P<0.05$) were selected for visual analysis. The significant rate (SR) represented the proportion of times where the influence of each meteorological factor on HFMD incidence was statistically significant at the 5% level.

R4.1.3 was used for basic statistical analysis and spatial autocorrelation detection. The models and procedures described in this study were implemented using an existing Python library available on GitHub. Specifically, we utilized the code from the MGTWR model repository maintained by Sunkun (2019). The repository can be accessed through https://github.com/sunkun1997/mgtwr . ArcGIS 10.8 was used for spatial data visualization.

Results

Description of HFMD

From January 1, 2015, to December 31, 2019, a total of 418,432 HFMD cases (0–15 years) were reported in Shandong Province. There were 255,618 male patients and 162,814 female patients, with an average male-to-female ratio of 1.57:1. Figure 2(a) shows the monthly distribution of the logarithm of CI_A during the study period, presenting a significant seasonality. The apparent peak of HFMD occurred from May to August, with a secondary peak in November. The two peaks accounted for 80.51% of all reported cases. Figure 2(b) displays the spatial distribution of CI_A (per 100,000 people). In central, northern, southern, and coastal regions, the CI_A might exceed 1500 per 100,000 people, while in counties with low incidence, it is less than 250 per 100,000 people. It can be seen that the distribution of HFMD in Shandong Province has spatial heterogeneity.

Table 1 shows that there was a high global spatial autocorrelation of HFMD in each epidemic year at the county level in Shandong Province from 2015 to 2019 (Moran's $I>0.35$, $P<0.001$). The results of local spatial autocorrelation are displayed in Fig. 2(c), indicating that the distribution of HFMD had obvious spatiotemporal characteristics. Except that most areas of Jinan City and some areas of Qingdao City were High-High cluster (HH) regions within 5 years, the distribution of Low-High outlier (LH) and Low-Low cluster (LL) regions varied with time. There were almost no High-Low outlier (HL) regions during the study period.

Description of meteorological factors

The results of Spearman correlation test are shown in Table 2. In this study, we considered the variables to be strongly correlated if their correlation coefficient ($|r|$) was 0.7 or higher [37]. Variables with such high correlation coefficients can lead to multicollinearity, which can inflate the variance of the coefficient estimates and make the model unstable. Therefore, to ensure the stability and interpretability of the model, we excluded SH and AP from the analysis due to their strong correlation with AT (r_S=-0.76 and 0.83, respectively).

Figure 3 shows the monthly distribution of meteorological factors from January 2015 to December 2019. The AT showed a clear cyclical pattern with significant seasonal variations. Peaks were observed annually, indicating higher temperatures in summer. The ARH fluctuated greatly over time, with lower values usually observed in spring. The AWS exhibited considerable variability over several months, with no clear cyclical or seasonal patterns. The TP showed significant seasonal peaks, primarily occurring in July and August.

Determining the optimum model and bandwidths

The model fitting evaluations of the MGTWR model, OLS model, and GTWR model are presented in Table 3. The GTWR model showed significant improvement over the OLS model, With the adjusted R^2 increasing from 0.43 to 0.81, the AICc decreasing from 28234.41 to 21180.57, and the RMSE decreasing from 1.35 to 0.66. Compared with the GTWR model, the adjusted R^2 of the MGTWR model increased from 0.81 to 0.92, while AICc and RMSE decreased from 21180.57 to 0.66 to 17965.28 and 0.41, respectively. It can be seen that the MGTWR model improved the model fitting.

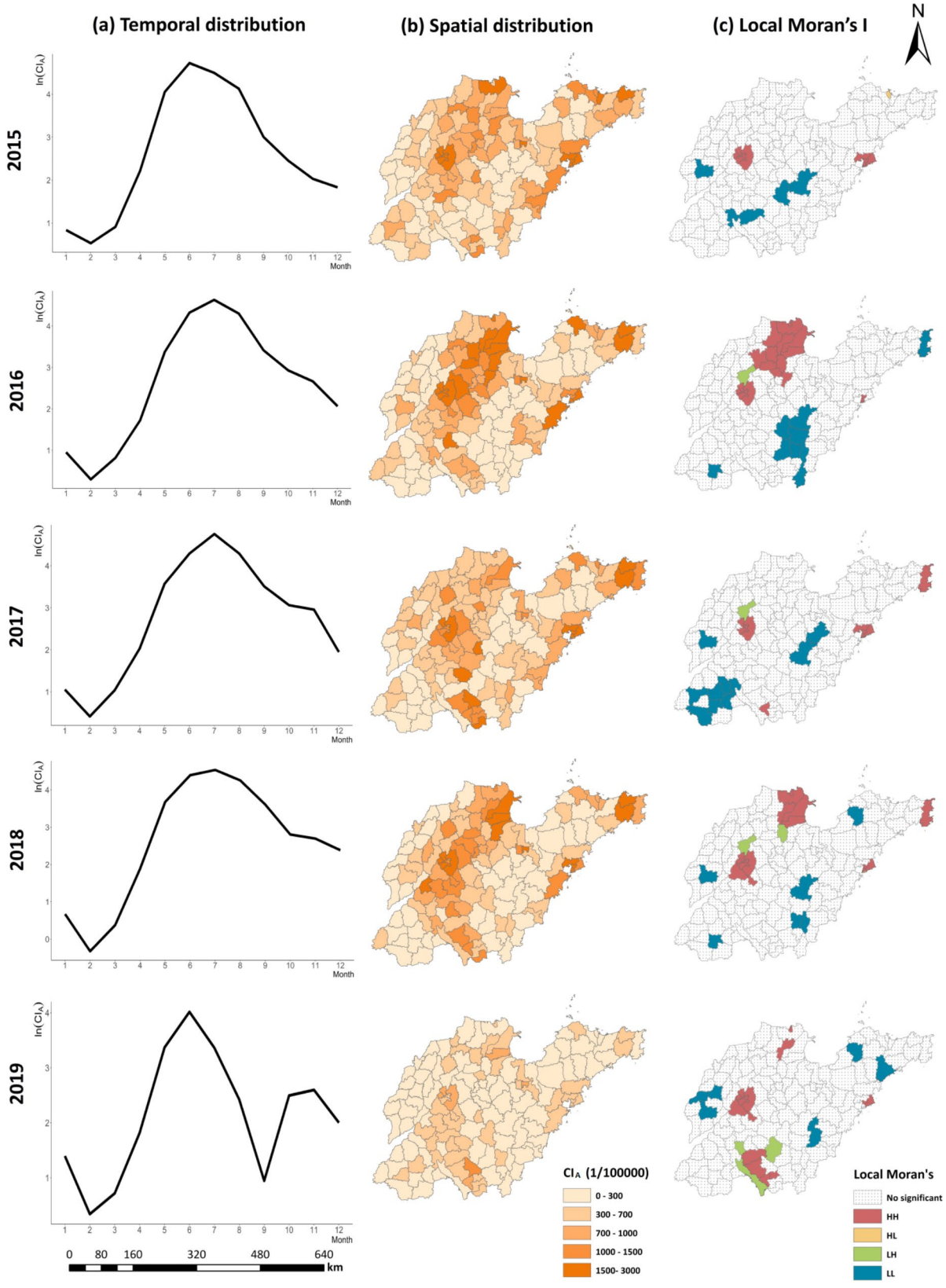

Fig. 2 Temporal and spatial distribution pattern of HFMD in Shandong Province, 2015–2019. The shading of the areas of Fig. 2(**b**) represents the HFMD incidence, with darker color of orange indicating higher incidence rates. The spatial autocorrelation of HFMD incidence is illustrated in Fig. 2(**c**), where different areas are colored based on clustering pattern.(Sources: http://www.geodata.cn/, the map was edited using ArcGIS 10.8)

Table 1 The global spatial autocorrelation analysis of HFMD cases in Shandong Province, 2015–2019

Year	Moran's I	Z-score	*P*-value
2015	0.44	8.51	< 0.001
2016	0.45	8.63	< 0.001
2017	0.36	7.01	< 0.001
2018	0.44	8.51	< 0.001
2019	0.37	7.18	< 0.001

Table 3 Performance evaluation of OLS, GTWR, and MGTWR models

Model	R^2	Adjusted R^2	AICc	RMSE
OLS	0.43	0.43	28234.31	1.35
GTWR	0.86	0.81	21180.57	0.66
MGTWR	0.95	0.92	17965.28	0.41

Note AICc represents the Akaike Information Criterion, and RMSE represents the root mean square error

Table 2 Spearman correlation coefficient between meteorological factors

Meteorological factors	AT	ARH	AP	TP	AWS	SH
AT	1					
ARH	0.45	1				
AP	-0.76	-0.31	1			
TP	0.68	0.64	-0.69	1		
AWS	-0.32	-0.57	0.21	-0.32	1	
SH	0.83	0.08	-0.75	0.60	0.02	1

Table 4 shows the bandwidths of the GTWR and MGTWR models. The GTWR model used fixed bandwidths, with temporal and spatial bandwidth sizes of 1.96 months and 57.50 km, respectively. The results of the MGTWR model showed that the temporal and spatial bandwidths of each meteorological factor were different, with the temporal bandwidths ranging from 1.48 months to 2.92 months and spatial bandwidths ranging from 20.73 km to 86.77 km, all of which did not exceed the maximum temporal and spatial scales of this study.

Effects of the meteorological factors on HFMD

As shown in Table 5, the parameters of the MGTWR model exhibit obvious spatiotemporal non-stationarity. Figure 4 illustrates the monthly SR of various meteorological factors affecting the HFMD incidence over 60 months. The SR for AT consistently exceeded 0.85 for most of the period. The impact of AT was most significant in the spring and summer months. The SR of ARH varied throughout the year, with the most significant effects observed during the summer months. On the contrary, in winter, its SR decreased. The impact of AWS was most notable in the autumn and early winter months, as indicated by the higher SR values during these periods. TP showed the most significant effects in the spring and summer months.

Figures 5, 6, 7 and 8 illustrate the spatial and temporal variations in the relationship between meteorological

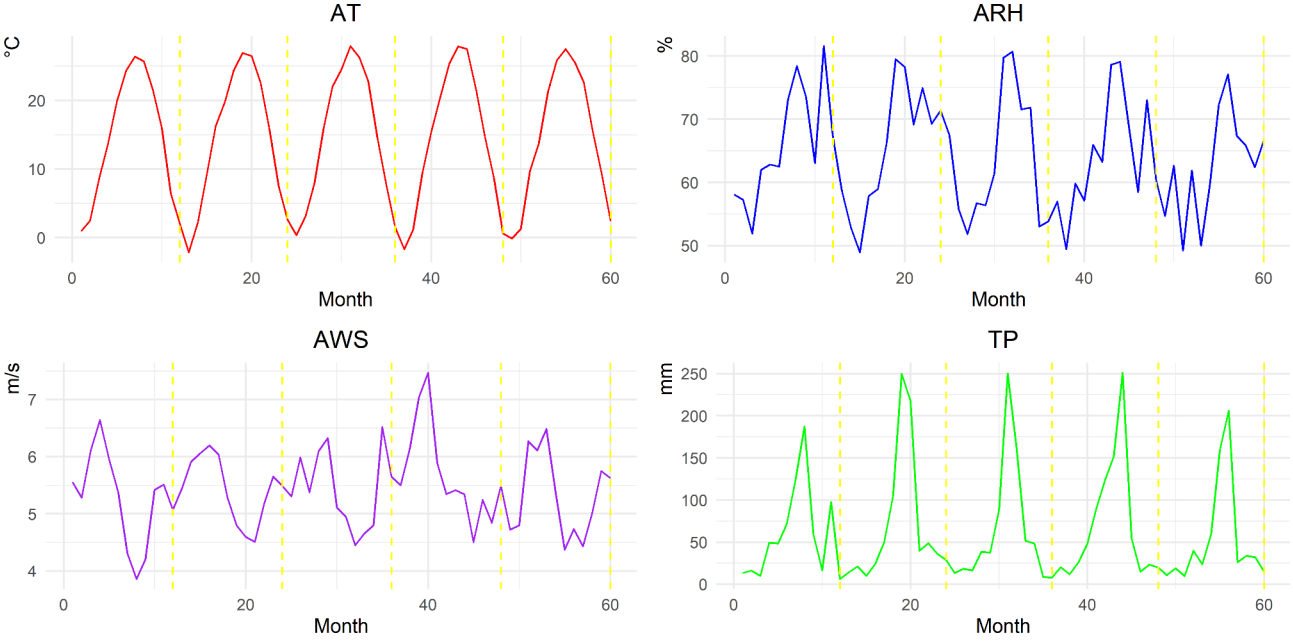

Fig. 3 Monthly distribution of meteorological factors

Table 4 Temporal and spatial bandwidths of GTWR and MGTWR models

Meteorological factors	MGTWR		GTWR	
	d_T (month)	d_S (km)	d_T (month)	d_S (km)
AT	2.92	37.27	1.96	57.50
ARH	1.57	86.77		
TP	1.48	79.34		
AWS	1.91	20.73		

Note d_T and d_S refer to the temporal bandwidth and spatial bandwidth, respectively. The maximum bandwidths of d_T and d_S are 60 months and 814.74 km, respectively

Table 5 Non-stationarity of parameters in the MGTWR model

Meteorological factors	F	*P*-Value
AT	13.90	<0.001
ARH	14.49	<0.001
TP	23.73	<0.001
AWS	39.53	<0.001

factors and HFMD incidences from January 2015 to December 2019. The influence of AT on HFMD was predominantly positive in most times and regions (Fig. 5). The coefficient was significantly higher in the peninsula region compared to other areas. In some months, a negative correlation appeared in the southwestern part of Shandong province.

The relationship between ARH and HFMD incidences was predominantly positive (Fig. 6). Spatially, the relationship in the Shandong Peninsula showed a consistent positive correlation most of the time, suggesting that higher ARH in this region was associated with an increase in HFMD cases. In contrast, the relationship in other regions displayed negative correlations only in certain winter months, indicating that higher humidity in these areas was associated with lower HFMD incidences during specific periods.

The influence of AWS on HFMD incidence was mainly negative in the central and southwestern regions of Shandong province (Fig. 7). The coefficient values for most counties were between −0.74 and 0. In some months, such as November 2016 to March 2017, a marked negative correlation was observed in the northwestern regions. Conversely, the HFMD incidence in the Shandong Peninsula increased with higher wind speeds most of the time.

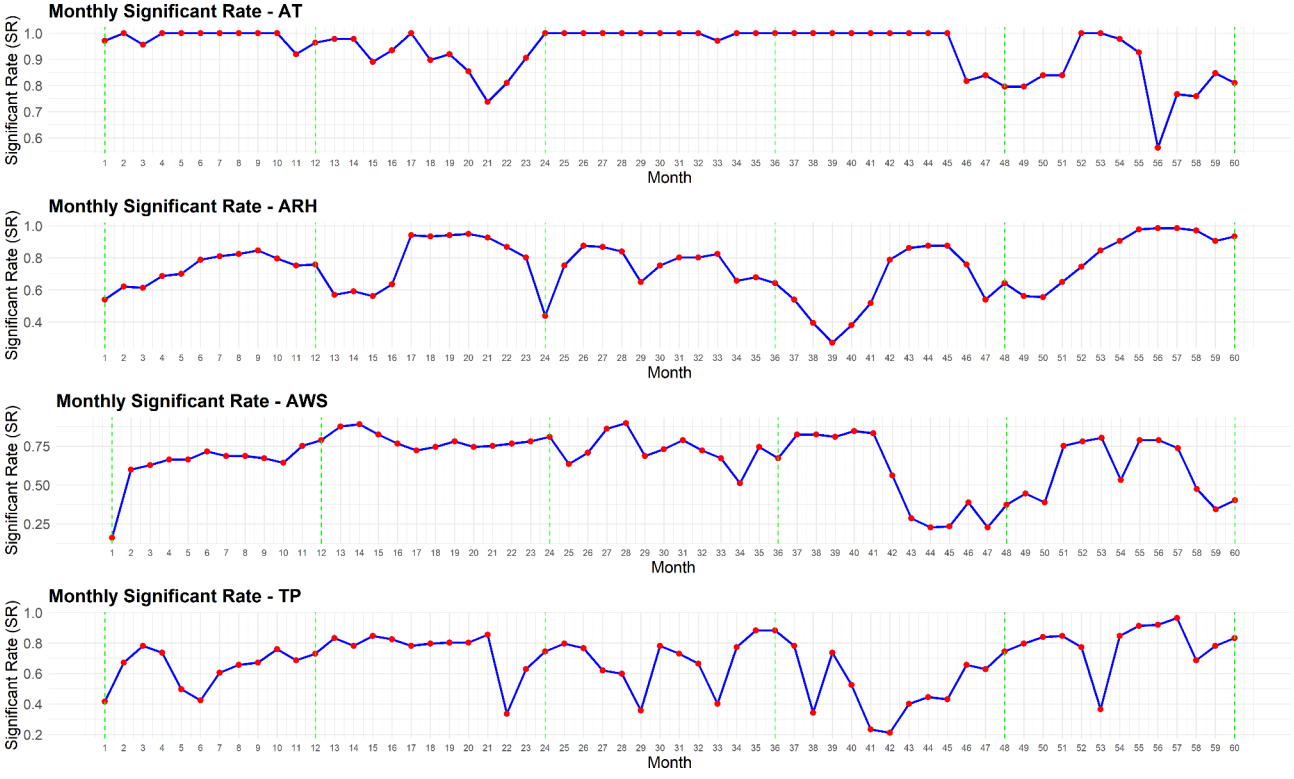

Fig. 4 Monthly Significant Rate Variation by Different Meteorological Factors

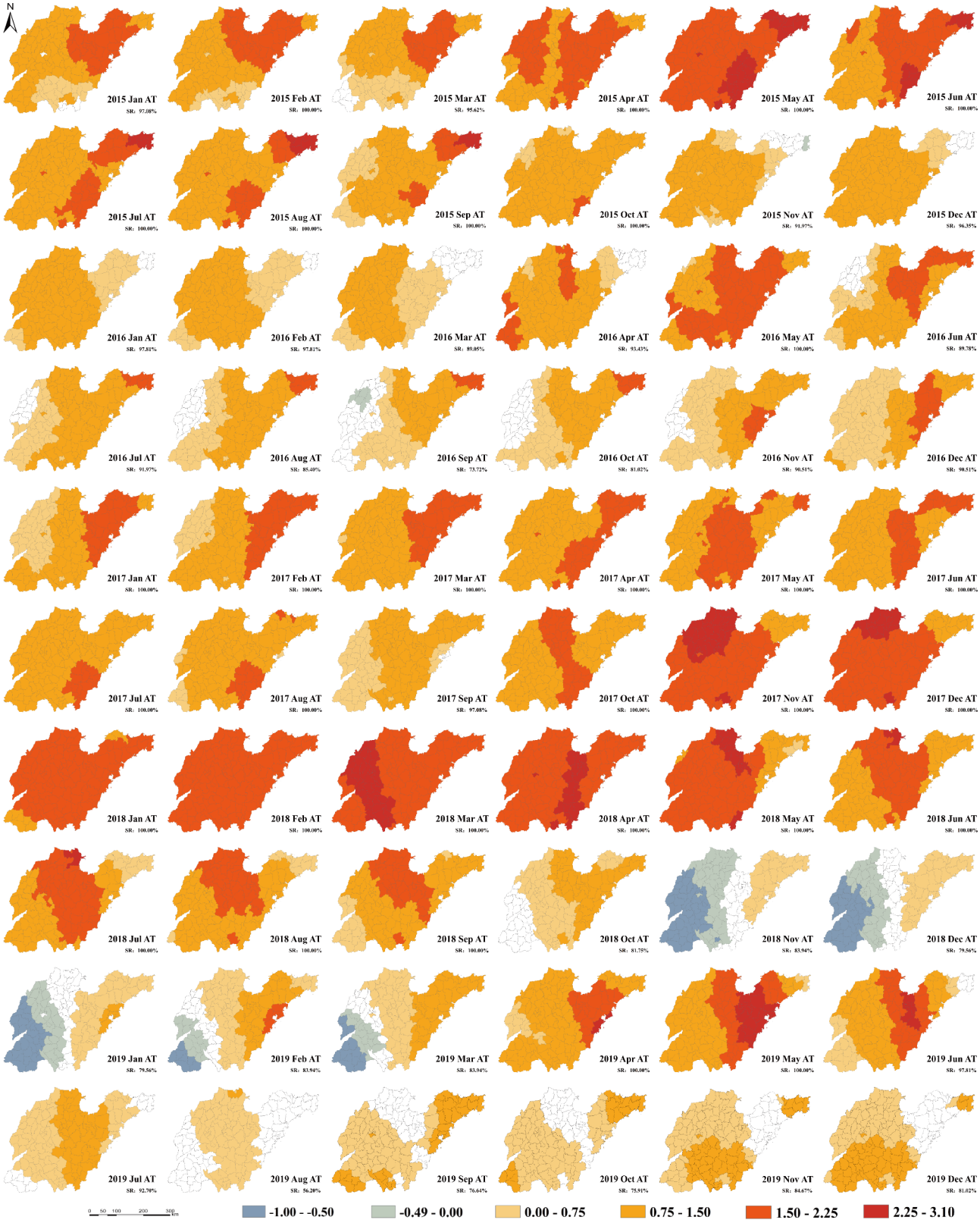

Fig. 5 Spatial variation of the estimated coefficient of AT from January 2015 to December 2019. Areas of the map with red color represent positive correlations and blue color represent negative correlations. The darker the color, the higher the absolute value of the correlation coefficient.(Sources: http://www.geodata.cn/, the map was edited using ArcGIS 10.8)

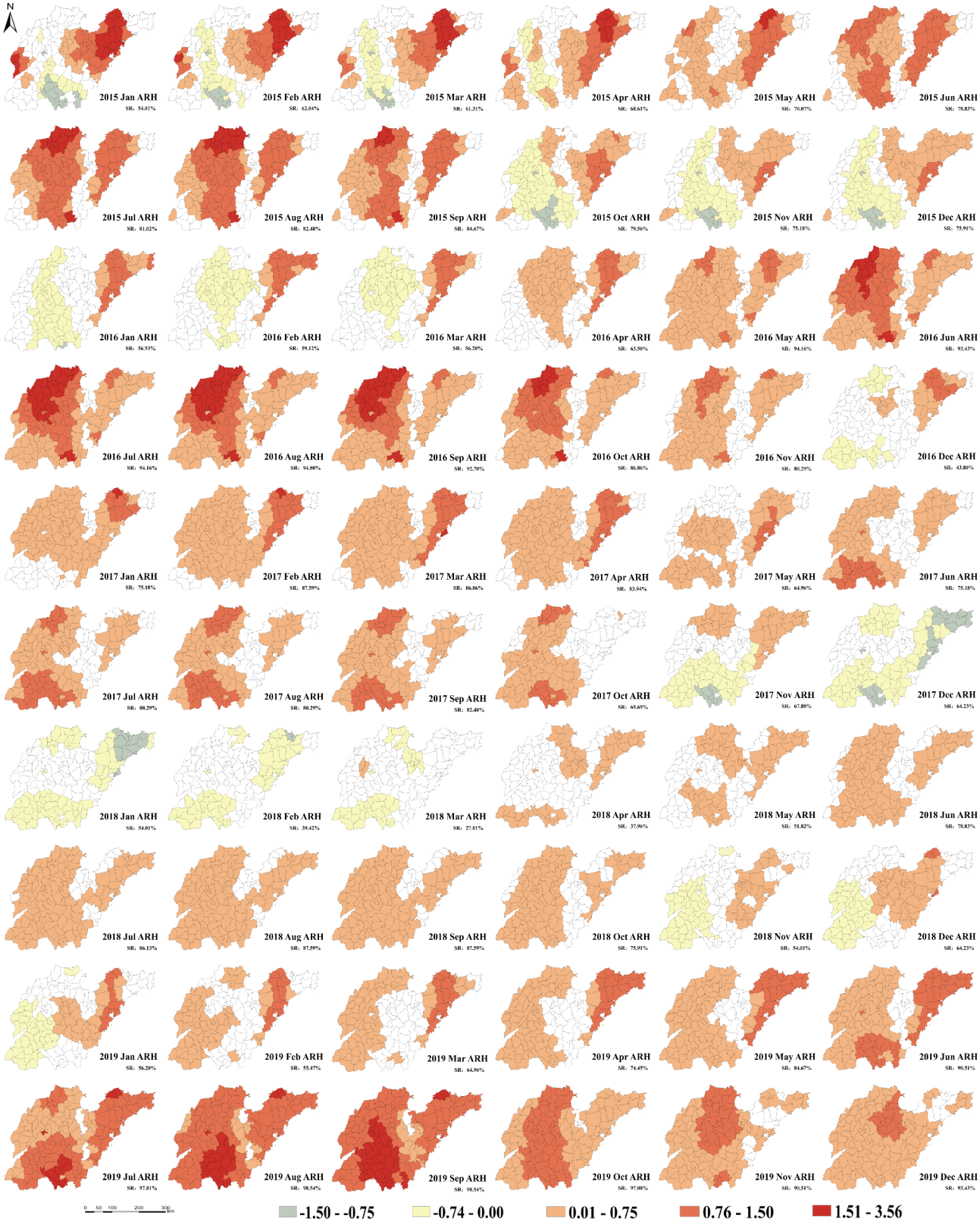

Fig. 6 Spatial variation of the estimated coefficient of ARH from January 2015 to December 2019. Areas of the map with red color represent positive correlations and blue color represent negative correlations. The darker the color, the higher the absolute value of the correlation coefficient.(Sources: http://www.geodata.cn/, the map was edited using ArcGIS 10.8)

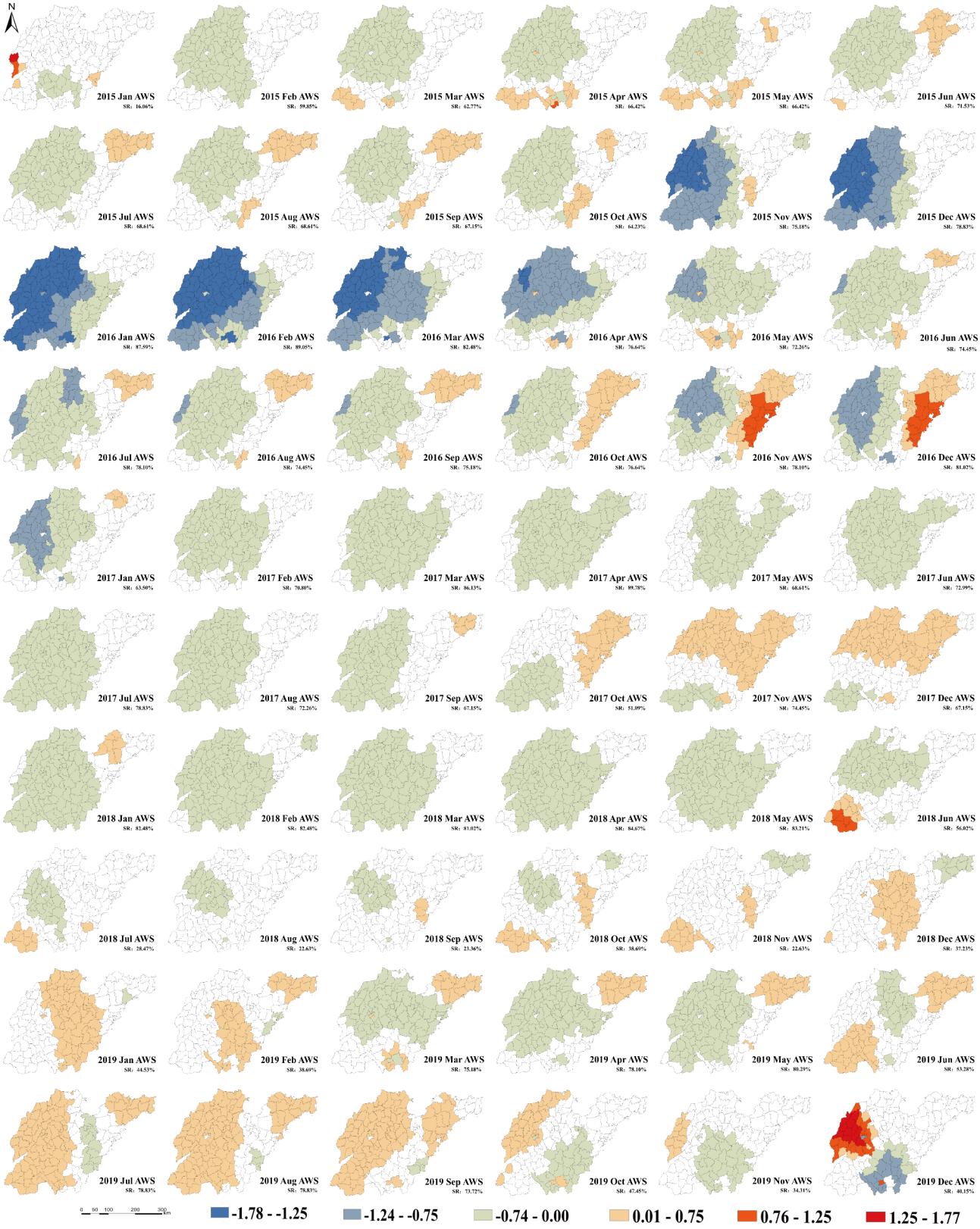

Fig. 7 Spatial variation of the estimated coefficient of AWS from January 2015 to December 2019. Areas of the map with red color represent positive correlations and blue color represent negative correlations. The darker the color, the higher the absolute value of the correlation coefficient.(Sources: http://www.geodata.cn/, the map was edited using ArcGIS 10.8)

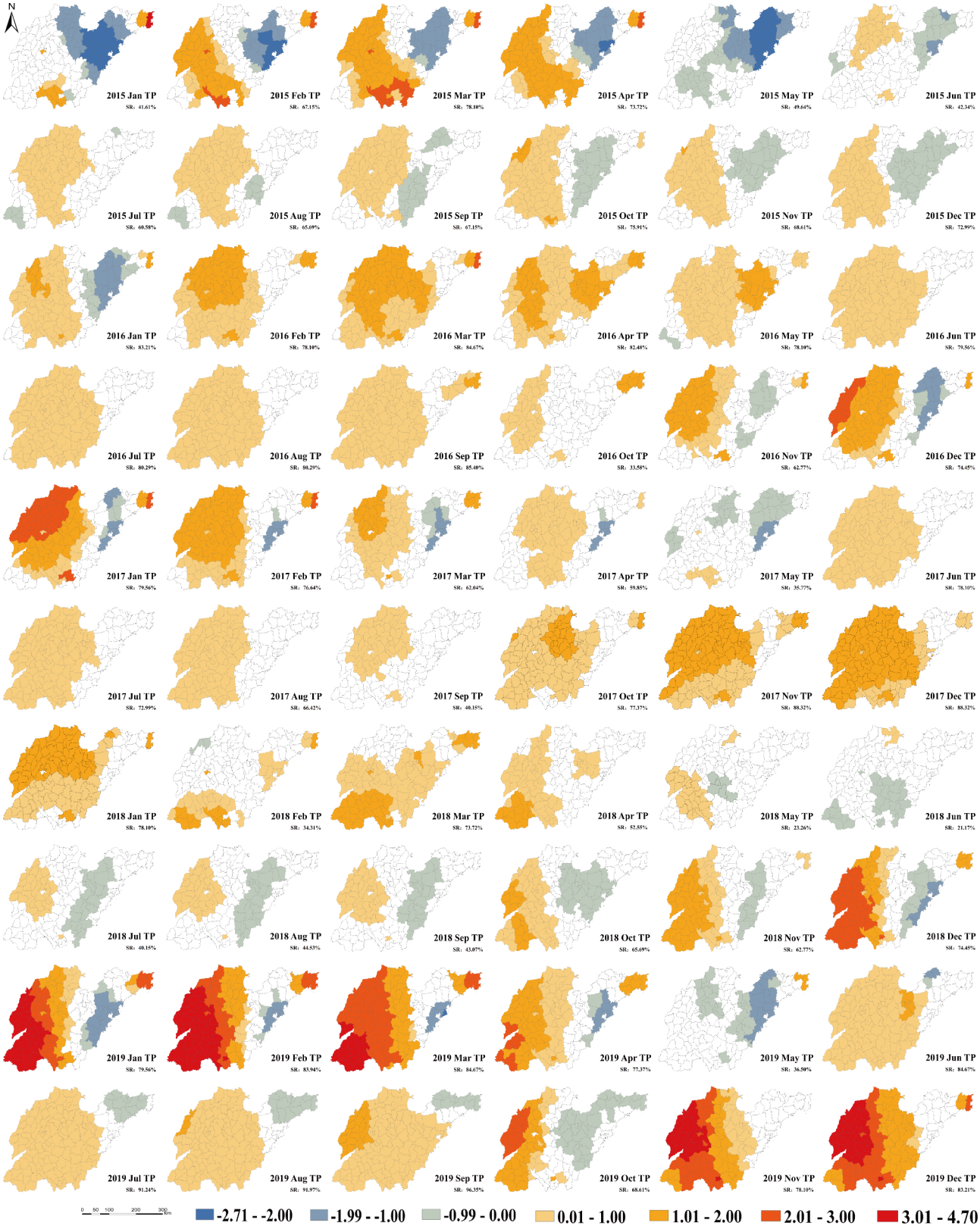

Fig. 8 Spatial variation of the estimated coefficient of TP from January 2015 to December 2019. Areas of the map with red color represent positive correlations and blue color represent negative correlations. The darker the color, the higher the absolute value of the correlation coefficient. (Sources: http://www.geodata.cn/, the map was edited using ArcGIS 10.8)

TP was significantly positively correlated with HFMD in most months, except for the peninsula region (Fig. 8). The influence of TP increased towards the western regions, with higher coefficients indicating a stronger positive correlation. In addition, the impact of TP on HFMD incidence was significantly higher in winter. Some coastal peninsula regions displayed negative correlations in some months, but they were unstable and may be associated with substantial temporal variations in precipitation.

Discussion

Shandong Province has been one of the most serious HFMD epidemic areas in China. The spatial autocorrelation test indicated that HFMD had significant spatial autocorrelation at the county level in Shandong Province. The occurrence of HFMD was seasonal, but it also had obvious spatial heterogeneity. A notable finding in our study was the overall lower CI_A in 2019 compared to other years. The sudden drop in HFMD incidence observed in September 2019 further highlights this anomaly. One reason is that the EV-A71 vaccine was first introduced in China in 2016 and widespread vaccination began in 2018. By the end of 2018, nearly 30% of children had received two doses of the vaccine, which has been proven highly effective in preventing infections, especially in children under five years old [38, 39]. This vaccination effort may explain the decline in cases observed in 2019. Additionally, the Local Moran's I analysis also revealed different patterns in the eastern Shandong Peninsula region in different years, with LL clusters in 2016 and HH clusters in 2017 and 2018. These patterns may indicate a shift in disease dynamics, possibly due to changes in environmental conditions, human behavior, or healthcare accessibility. The LL pattern in 2016 suggests a period of lower incidence in these areas, potentially due to effective control measures or lower transmission rates. In contrast, the HH patterns in 2017 and 2018 could be due to outbreaks or increased transmission rates influenced by factors such as high temperatures and humidity, which are conducive to the spread of HFMD virus.

In this study, the MGTWR model was used to investigate the impact of meteorological factors on the transmission of HFMD from a spatiotemporal perspective. By comparing with the traditional OLS model and GTWR model, we found that the MGTWR model had great improvements in model explanatory power and model fitting. This further indicates that classical statistical methods may have certain biases without considering spatial autocorrelation.

Based on the coefficient estimates of the MGTWR model, some informative spatiotemporal patterns of the influence of meteorological factors on HFMD have been revealed. We found that the impact of AT on HFMD was predominantly positive within one year, and the influence intensity and SR were greater than other factors, which was consistent with previous studies on the effect of AT [7, 40, 41]. Studies have shown that high temperatures can facilitate the transmission of enteroviruses by enhancing viral survival and reproduction rates [42, 43]. In addition, warmer weather increases children's outdoor activities, which leads to close contact between them. The spatial variation of the coefficients suggests that the impact of temperature on HFMD is not uniform in different regions, which may be related to the differences in local climate conditions and population density. The occurrence of negative correlations may be related to the interaction between extreme climate conditions and various meteorological factors. For instance, extreme weather conditions, such as low humidity combined with high temperatures, can create an unfavorable environment for the virus or restrict children's activities, thereby reducing transmission rates. The spatial heterogeneity of relationship between temperature and HFMD underscores the importance of considering local environmental factors in disease prevention and control strategies. For example, the impact of temperature on HFMD in a certain region is more significant than in other regions, indicating that local climatic and environmental factors may amplify the effect of temperature on HFMD transmission.

The spatiotemporal patterns of the relationship between ARH and HFMD observed in this study can be explained by several factors. Firstly, the overall positive correlation suggests that a higher ARH generally creates favorable conditions for the survival and transmission of the HFMD virus. The virus tends to thrive in more humid environments, which can facilitate its spread through respiratory droplets and contact with contaminated surfaces [44]. Secondly, the consistent positive correlation in the Shandong Peninsula can be attributed to climatic and environmental conditions in the region, which are conducive to the spread of HFMD. Coastal climate typically features high ARH levels, which, combined with dense populations and high mobility, can enhance the transmission of the virus. Thirdly, in certain winter months, the negative correlations observed in other regions may be due to the combined effects of low temperatures and high humidity, which could limit outdoor activities and reduce contact between children. Despite high ARH levels, this seasonal effect may reduce the chances of HFMD transmission.

The predominantly positive correlation between TP and HFMD suggests that higher rainfall generally leads to an increase in HFMD cases. Increased precipitation can create more favorable conditions for the transmission of enteroviruses that cause HFMD. Rainfall can enhance the survival and spread of these viruses in the environment, especially in regions with inadequate sanitation

and drainage systems. This is supported by studies such as those by Koh et al. [45], which highlight the role of climatic conditions in HFMD outbreaks in Asia. Furthermore, high precipitation could promote virus attachment to small particles in the air, toys, and food, thus increasing the risk of HFMD [42]. The observed patterns indicate that the HFMD incidences are high in regions with significant precipitation in winter, which may indeed be related to the combined effects of cold and humid environments on human immune function [46]. Cold and humid conditions can influence the immune system in various ways, potentially increasing susceptibility to infections such as HFMD. The negative correlations observed in certain coastal peninsula areas in specific months are less stable, which may be due to the variability in precipitation patterns in these regions. These areas may experience sudden changes in rainfall, which may disrupt the typical relationship between precipitation and HFMD incidence.

The results indicate that wind speed plays a significant role in the incidence of HFMD, and generally the higher the wind speeds, the lower the incidence. This finding is consistent with some studies that suggest higher AWS can disperse airborne pathogens and reduce the likelihood of person-to-person transmission of enteroviruses [47, 48]. In addition, windy weather might reduce outdoor activities, thus reducing the chance of exposure to the virus. The positive correlation between AWS and HFMD incidence in the peninsular regions can be attributed to several unique factors. Coastal areas consistently experience higher wind speeds and have higher population densities. Increased wind speeds facilitate the airborne transmission of the virus among dense populations. This is consistent with the research of Dong et al. [49], which reported a positive correlation in Beijing. Moreover, many coastal regions are popular tourist destinations, leading to high population mobility, which further enhances the spread of HFMD. This aligns with the findings of Zhang et al. and Yang et al. [50, 51], who also noted the significant impact of human mobility and density on disease transmission in these regions.

This study underscored the importance of incorporating both spatial and temporal dimensions in understanding the epidemiological dynamics of HFMD. Future research should continue to explore the complex interactions between meteorological factors and infectious diseases, utilizing advanced spatial-temporal models like MGTWR to inform public health interventions and policies. However, this study also has several limitations worth mentioning. Firstly, this study only analyzed the association between HFMD and meteorological factors and did not consider socioeconomic, behavioral, or physiological influencing factors. Secondly, as an ecological study, the complex impact between climatic factors and HFMD transmission may vary significantly across different regions. Therefore, our results should be cautiously extrapolated to areas with different climatic and socio-environmental conditions.

Conclusions

This study confirmed that the spatial and temporal distribution of HFMD varied at county scales. The MGTWR model was used to explore the influence of meteorological factors on the incidence of HFMD, which provides a new method for future studies on HFMD and other diseases. Although the complexity of HFMD could not be fully explained by meteorological factors, our results provided new quantitative evidence, indicating the effect of meteorological factors on HFMD at a finer spatial-temporal scale. The results can help public health authorities prioritize prevention and control measures in different regions and weather conditions, and provide guidance for the government to rationally allocate public health resources.

Abbreviations

HFMD	Hand, Foot and Mouth Disease
EV-A71	Enterovirus 71
CV-A16	Coxsackievirus A16
OLS	Ordinary Least Squares
GWR	Geographically Weighted Regression
GTWR	Geographically and Temporally Weighted Regression
MGTWR	Multiscale Geographically and Temporally Weighted Regression
CISDCP	China Information System for Disease Control and Prevention
CI	Cumulative Incidence
MCMC	Monte Carlo Markov Chain
CI_A	Adjusted Cumulative Incidence
AT	Average Temperature
ARH	Average Relative Humidity
AP	Average Air Pressure
TP	Total Precipitation
AWS	Average Wind Speed
SH	Sunshine Hours
SOC	Change of Score
AICc	Average Air Pressure
RMSE	Root Mean Square Error
SR	Rate of significance
HH	High-High cluster
LH	Low-High outlier
LL	Low-Low cluster
HL	High-Low outlier

Supplementary Information

The online version contains supplementary material available at https://doi.org/10.1186/s12889-024-20596-5.

Supplementary Material 1

Acknowledgements

The authors would like to thank the Shandong Centers for Disease Control and Prevention (CDC) for providing HFMD data. The authors also thank the China Meteorological Data Sharing Service System for providing meteorological data for all analyses in the present study.

Author contributions
YX.L. conceived the original study idea, and led the study. C.Z. and Z.K. developed statistical analysis and preparation of the manuscript. F.H. and X.W. developed data interpretation and revision of manuscript. Y.F., Y.L., and D.S. revised the manuscript. Y.Z and R.Z prepared Figs. 1, 2, 3, 4, 5, 6, 7 and 8. All the authors contributed to and approved the final manuscript.

Funding
This study was funded by a grant from the National Major project of the Science and Technology Ministry during the 13th Five-year Plan Period [No.2017ZX10104001], and the Shandong Medical and Health Science and Technology Development Project [No.2019WS433].

Data availability
The digital map data can be accessed at http://www.geodata.cn/. The meteorological data of this study can be accessed at https://data.cma.cn/.

Declarations

Ethics approval and consent to participate
This research involved human data on cases of HFMD have been performed in accordance with the Declaration of Helsinki and approved by the Shandong Center for Disease Control and Prevention ethics committee. Shandong Center for Disease Control and Prevention granted permission to use the data in the study. The data were anonymized before its use and did not contain any personal information, it can be obtained from the Shandong Center for Disease Control and Prevention upon reasonable request.

Consent for publication
Not applicable.

Competing interests
The authors declare no competing interests.

Received: 15 March 2023 / Accepted: 1 November 2024
Published online: 12 November 2024

References

1. Gopalkrishna V, Patil PR, Patil GP, Chitambar SD. Circulation of multiple enterovirus serotypes causing hand, foot and mouth disease in India. J Med Microbiol. 2012;61(Pt 3):420–5. https://doi.org/10.1099/jmm.0.036400-0.
2. Yang F, Zhang T, Hu Y, Wang X, Du J, Li Y, Sun S, Sun X, Li Z, Jin Q. Survey of enterovirus infections from hand, foot and mouth disease outbreak in China, 2009. Virol J. 2011;8:508. https://doi.org/10.1186/1743-422X-8-508.
3. Cardosa MJ, Perera D, Brown BA, Cheon D, Chan HM, Chan KP, Cho H, McMinn P. Molecular epidemiology of human enterovirus 71 strains and recent outbreaks in the Asia-Pacific region: comparative analysis of the VP1 and VP4 genes. Emerg Infect Dis. 2003;9(4):461–8. https://doi.org/10.3201/eid0904.020395.
4. Fan X, Jiang J, Liu Y, Huang X, Wang P, Liu L, Wang J, Chen W, Wu W, Xu B. Detection of human enterovirus 71 and Coxsackievirus A16 in an outbreak of hand, foot, and mouth disease in Henan Province, China in 2009. Virus Genes. 2013;46(1):1–9. https://doi.org/10.1007/s11262-012-0814-x.
5. Zeng M, Li YF, Wang XH, Lu GP, Shen HG, Yu H, Zhu QR. Epidemiology of hand, foot, and mouth disease in children in Shanghai 2007–2010. Epidemiol Infect. 2012;140(6):1122–30. https://doi.org/10.1017/s0950268811001622.
6. Ji T, Han T, Tan X, Zhu S, Yan D, Yang Q, Song Y, Cui A, Zhang Y, Mao N, et al. Surveillance, epidemiology, and pathogen spectrum of hand, foot, and mouth disease in mainland of China from 2008 to 2017. Biosaf Health. 2019;1(1):32–40. https://doi.org/10.1016/j.bsheal.2019.02.005.
7. Onozuka D, Hashizume M. The influence of temperature and humidity on the incidence of hand, foot, and mouth disease in Japan. Sci Total Environ. 2011;410–411:119–25. https://doi.org/10.1016/j.scitotenv.2011.09.055.
8. Qi H, Chen Y, Xu D, Su H, Zhan L, Xu Z, Huang Y, He Q, Hu Y, Lynn H, et al. Impact of meteorological factors on the incidence of childhood hand, foot, and mouth disease (HFMD) analyzed by DLNMs-based time series approach. Infect Dis Poverty. 2018;7(1):7. https://doi.org/10.1186/s40249-018-0388-5.
9. Li J, Zhang X, Wang L, Xu C, Xiao G, Wang R, Zheng F, Wang F. Spatial-temporal heterogeneity of hand, foot and mouth disease and impact of meteorological factors in arid/ semi-arid regions: a case study in Ningxia, China. BMC Public Health. 2019;19(1):1482. https://doi.org/10.1186/s12889-019-7758-1.
10. Peng H, Chen Z, Cai L, Liao J, Zheng K, Li S, Ren X, Duan X, Tang X, Wang X, et al. Relationship between meteorological factors, air pollutants and hand, foot and mouth disease from 2014 to 2020. BMC Public Health. 2022;22(1):998. https://doi.org/10.1186/s12889-022-13365-9.
11. Xie L, Huang R, Wang H, Liu S. Spatial-temporal heterogeneity and meteorological factors of hand-foot-and-mouth disease in Xinjiang, China from 2008 to 2016. PLoS ONE. 2021;16(8):e0255222. https://doi.org/10.1371/journal.pone.0255222.
12. Hong Z, Hao H, Li C, Du W, Wei L, Wang H. Exploration of potential risks of Hand, Foot, and Mouth Disease in Inner Mongolia Autonomous Region, China using geographically weighted regression model. Sci Rep. 2018;8(1):17707. https://doi.org/10.1038/s41598-018-35721-9.
13. Yi S, Wang H, Yang S, Xie L, Gao Y, Ma C. Spatial and temporal characteristics of Hand-Foot-and-Mouth Disease and its response to climate factors in the Ili River Valley Region of China. Int J Environ Res Public Health. 2021;18(4). https://doi.org/10.3390/ijerph18041954.
14. Pearce MSJSTB. Geographically weighted regression: A method for exploring spatial nonstationarity. 1999, 8.
15. Huang B, Wu B, Barry M. Geographically and temporally weighted regression for modeling spatio-temporal variation in house prices. Int J Geogr Inf Sci. 2010;24(3):383–401. https://doi.org/10.1080/13658810802672469.
16. Chen Y, Chen M, Huang B, Wu C, Shi W. Modeling the Spatiotemporal Association Between COVID-19 Transmission and Population Mobility Using Geographically and Temporally Weighted Regression. *GeoHealth* 2021, 5(5):e2021GH000402. https://doi.org/10.1029/2021gh000402
17. Ge L, Zhao Y, Sheng Z, Wang N, Zhou K, Mu X, Guo L, Wang T, Yang Z, Huo X. Construction of a Seasonal difference-geographically and temporally weighted regression (SD-GTWR) model and comparative analysis with GWR-Based models for hemorrhagic fever with renal syndrome (HFRS) in Hubei Province (China). Int J Environ Res Public Health. 2016;13(11). https://doi.org/10.3390/ijerph13111062.
18. Mollalo A, Vahedi B, Rivera KM. GIS-based spatial modeling of COVID-19 incidence rate in the continental United States. Sci Total Environ. 2020;728:138884. https://doi.org/10.1016/j.scitotenv.2020.138884.
19. Wang F, Liu X, Bergquist R, Lv X, Liu Y, Gao F, Li C, Zhang Z. Bayesian maximum entropy-based prediction of the spatiotemporal risk of schistosomiasis in Anhui Province, China. BMC Infect Dis. 2021;21(1):1171. https://doi.org/10.1186/s12879-021-06854-6.
20. Wu C, Ren F, Hu W, Du Q. Multiscale geographically and temporally weighted regression: exploring the spatiotemporal determinants of housing prices. Int J Geogr Inf Sci. 2019;33(3):489–511. https://doi.org/10.1080/13658816.2018.1545158.
21. Wu Y, Wang T, Zhao M, Dong S, Wang S, Shi J. Spatiotemporal cluster patterns of hand, foot, and mouth disease at the province level in mainland China, 2011–2018. PLoS ONE. 2022;17(8):e0270061. https://doi.org/10.1371/journal.pone.0270061.
22. Bo YC, Song C, Wang JF, Li XW. Using an autologistic regression model to identify spatial risk factors and spatial risk patterns of hand, foot and mouth disease (HFMD) in Mainland China. BMC Public Health. 2014;14:358. https://doi.org/10.1186/1471-2458-14-358.
23. Li T, Yang Z, Liu X, Kang Y, Wang M. Hand-foot-and-mouth disease epidemiological status and relationship with meteorological variables in Guangzhou, southern China, 2008–2012. Rev Inst Med Trop Sao Paulo. 2014;56(6):533–9. https://doi.org/10.1590/s0036-46652014000600014.
24. Zhang Z, Xie X, Chen X, Li Y, Lu Y, Mei S, Liao Y, Lin H. Short-term effects of meteorological factors on hand, foot and mouth disease among children in Shenzhen, China: non-linearity, threshold and interaction. Sci Total Environ. 2016;539:576–82. https://doi.org/10.1016/j.scitotenv.2015.09.027.
25. Hong Z, Mei C, Wang H, Du W. Spatiotemporal effects of climate factors on childhood hand, foot, and mouth disease: a case study using mixed geographically and temporally weighted regression models. Int J Geogr Inf Sci. 2021;35(8):1611–33. https://doi.org/10.1080/13658816.2021.1882681.
26. Liu L, Wang L, Qi C, Zhu Y, Li C, Jia Y, She K, Liu T, Zhang Y, Cui F, et al. Epidemiological characteristics and spatiotemporal analysis of hand-foot-mouth diseases from 2010 to 2019 in Zibo City, Shandong, China. BMC Public Health. 2021;21(1):1640. https://doi.org/10.1186/s12889-021-11665-0.
27. Liu Y, Wang X, Liu Y, Sun D, Ding S, Zhang B, Du Z, Xue F. Detecting spatial-temporal clusters of HFMD from 2007 to 2011 in Shandong Province, China. PLoS ONE. 2013;8(5):e63447. https://doi.org/10.1371/journal.pone.0063447.

28. Li XW, Ni X, Qian SY, Wang Q, Jiang RM, Xu WB, Zhang YC, Yu GJ, Chen Q, Shang YX, et al. Chinese guidelines for the diagnosis and treatment of hand, foot and mouth disease (2018 edition). World J Pediatr. 2018;14(5):437–47. https://doi.org/10.1007/s12519-018-0189-8.
29. Haining R, editor. Spatial Data Analysis: Theory and Practice2003.
30. Lawson AB, Browne WJ, Rodeiro CLV, editors. Disease Mapping with WinBUGS and MLwiN2003.
31. Lee TCM. Smoothing parameter selection for smoothing splines: a simulation study. Comput Stat Data Anal. 2003;42(1):139–48. https://doi.org/10.1016/S0167-9473(02)00159-7.
32. Fotheringham AS, Yang W, Kang W. Multiscale geographically weighted regression (MGWR). Annals Am Association Geographers. 2017;107(6):1247–65. https://doi.org/10.1080/24694452.2017.1352480.
33. Anselin LJGA. Local Indicators of Spatial Association—LISA. 2010, 27:93–115.
34. Dong F, Zhang S, Long R, Zhang X, Sun Z. Determinants of haze pollution: an analysis from the perspective of spatiotemporal heterogeneity. J Clean Prod. 2019;222:768–83. https://doi.org/10.1016/j.jclepro.2019.03.105.
35. Xuan H, Li S, Amin M. STATISTICAL INFERENCE OF GEOGRAPHICALLY AND TEMPORALLY WEIGHTED REGRESSION MODEL. In: *2015*; 2015.
36. Fotheringham A, Brunsdon C, Charlton M. Geographically weighted regression: the analysis of spatially varying relationships. Wiley; 2002. p. 13.
37. Cohen JJTSEoRD. Statistical Power Analysis for the Behavioral Sciences. 1988.
38. Ye L, Chen J, Fang T, Ma R, Wang J, Pan X, Dong H, Xu G. Vaccination coverage estimates and utilization patterns of inactivated enterovirus 71 vaccine post vaccine introduction in Ningbo, China. BMC Public Health. 2021;21(1):1118. https://doi.org/10.1186/s12889-021-11198-6.
39. Jiang L, Jiang H, Tian X, Xia X, Huang T. Epidemiological characteristics of hand, foot, and mouth disease in Yunnan Province, China, 2008–2019. BMC Infect Dis. 2021;21(1):751. https://doi.org/10.1186/s12879-021-06462-4.
40. Zhang X, Xu C, Xiao G. Spatial heterogeneity of the association between temperature and hand, foot, and mouth disease risk in metropolitan and other areas. Sci Total Environ. 2020;713:136623. https://doi.org/10.1016/j.scitotenv.2020.136623.
41. Zhuang D, Hu W, Ren H, Ai W, Xu X. The influences of temperature on spatiotemporal trends of hand-foot-and-mouth disease in mainland China. Int J Environ Health Res. 2014;24(1):1–10. https://doi.org/10.1080/09603123.2013.769206.
42. Kung Y-H, Huang S-W, Kuo P-H, Kiang D, Ho M-S, Liu C-C, Yu C-K, Su I-J, Wang J-R. Introduction of a strong temperature-sensitive phenotype into enterovirus 71 by altering an amino acid of virus 3D polymerase. Virology. 2010;396(1):1–9. https://doi.org/10.1016/j.virol.2009.10.017.
43. Rzezutka A, Cook N. Survival of human enteric viruses in the environment and food. FEMS Microbiol Rev. 2004;28(4):441–53. https://doi.org/10.1016/j.femsre.2004.02.001.
44. Huang DC, Wang JF. Monitoring hand, foot and mouth disease by combining search engine query data and meteorological factors. Sci Total Environ. 2018;612:1293–9. https://doi.org/10.1016/j.scitotenv.2017.09.017.
45. Koh WM, Bogich T, Siegel K, Jin J, Chong EY, Tan CY, Chen MI, Horby P, Cook AR. The epidemiology of Hand, Foot and Mouth Disease in Asia: a systematic review and analysis. Pediatr Infect Dis J. 2016;35(10):e285–300. https://doi.org/10.1097/INF.0000000000001242.
46. Knorr-Held L. Bayesian modelling of inseparable space-time variation in disease risk. Stat Med. 2000;19(17–18):2555–67. https://doi.org/10.1002/1097-0258(20000915/30)19:17/18<2555::aid-sim587>3.0.co;2-#.
47. Cai W, Luo C, Geng X, Zha Y, Zhang T, Zhang H, Yang C, Yin F, Ma Y, Shui T. City-level meteorological conditions modify the relationships between exposure to multiple air pollutants and the risk of pediatric hand, foot, and mouth disease in the Sichuan Basin, China. Front Public Health. 2023;11:1140639. https://doi.org/10.3389/fpubh.2023.1140639.
48. Yu G, Li Y, Cai J, Yu D, Tang J, Zhai W, Wei Y, Chen S, Chen Q, Qin J. Short-term effects of meteorological factors and air pollution on childhood hand-foot-mouth disease in Guilin, China. Sci Total Environ. 2019;646:460–70. https://doi.org/10.1016/j.scitotenv.2018.07.329.
49. Dong W, Li X, Yang P, Liao H, Wang X, Wang Q. The effects of Weather factors on Hand, Foot and Mouth Disease in Beijing. Sci Rep. 2016;6:19247. https://doi.org/10.1038/srep19247.
50. Liu Y, Wang X, Pang C, Yuan Z, Li H, Xue F. Spatio-temporal analysis of the relationship between climate and hand, foot, and mouth disease in Shandong province, China, 2008–2012. BMC Infect Dis. 2015;15:146. https://doi.org/10.1186/s12879-015-0901-4.
51. Liu Y, Feng Z, Song Y. The impacts of meteorological factors on the incidence of hand, foot, and mouth disease in China: an interactive perspective. Appl Geogr. 2023;160:103092. https://doi.org/10.1016/j.apgeog.2023.103092.

Publisher's note